

Lawrence Berkeley National Laboratory

LBL Publications

Title

Increased extreme rains intensify erosional nitrogen and phosphorus fluxes to the northern Gulf of Mexico in recent decades

Permalink

<https://escholarship.org/uc/item/4g4511q4>

Journal

Environmental Research Letters, 16(5)

ISSN

1748-9318

Authors

Tan, Zeli
Leung, L Ruby
Li, Hong-Yi
[et al.](#)

Publication Date

2021-05-01

DOI

10.1088/1748-9326/abf006

Peer reviewed

LETTER • OPEN ACCESS

Increased extreme rains intensify erosional nitrogen and phosphorus fluxes to the northern Gulf of Mexico in recent decades

To cite this article: Zeli Tan *et al* 2021 *Environ. Res. Lett.* **16** 054080

View the [article online](#) for updates and enhancements.

ENVIRONMENTAL RESEARCH
LETTERS

LETTER

OPEN ACCESS

RECEIVED
18 November 2020REVISED
16 March 2021ACCEPTED FOR PUBLICATION
18 March 2021PUBLISHED
14 May 2021

Original content from
this work may be used
under the terms of the
[Creative Commons
Attribution 4.0 licence](#).

Any further distribution
of this work must
maintain attribution to
the author(s) and the title
of the work, journal
citation and DOI.



Increased extreme rains intensify erosional nitrogen and phosphorus fluxes to the northern Gulf of Mexico in recent decades

Zeli Tan^{1,*}, L Ruby Leung¹, Hong-Yi Li², Teklu Tesfa¹, Qing Zhu³, Xiaojuan Yang⁴, Ying Liu¹ and Maoyi Huang¹¹ Pacific Northwest National Laboratory, Richland, WA, United States of America² Department of Civil and Environmental Engineering, University of Houston, Houston, TX, United States of America³ Climate and Ecosystem Sciences Division, Climate Sciences Department, Lawrence Berkeley National Laboratory, Berkeley, CA, United States of America⁴ Oak Ridge National Laboratory, Oak Ridge, TN, United States of America

* Author to whom any correspondence should be addressed.

E-mail: zeli.tan@pnnl.gov**Keywords:** soil erosion, particulate phosphorus, particulate nitrogen, eutrophication, the northern Gulf of Mexico, extreme rainfallSupplementary material for this article is available [online](#)**Abstract**

Soil erosion delivers enormous amounts of macro-nutrients including nitrogen (N) and phosphorus (P) from land to rivers, potentially sustaining water column bioavailable nutrient levels for decades. In this study, we represent erosional N and P fluxes in the Energy Exascale Earth System Model (E3SM) and apply the model to the continental United States. We estimate that during 1991–2019 soil erosion delivers 775 Gg yr⁻¹ (1 Gg = 10⁹ g) of particulate N (PN) and 328 Gg yr⁻¹ of particulate P (PP) on average to the drainage basins of the northern Gulf of Mexico, including the Mississippi/Atchafalaya River and other rivers draining to the Texas Gulf and the Eastern Gulf. Our model simulation shows that in these rivers PP is the dominant P constituent and over 55% of P exported by erosion comes from soil P pools that could become bioavailable within decades. More importantly, we find that during 1991–2019 erosional N and P fluxes increase at rates of about 15 Gg N yr⁻¹ and 6 Gg P yr⁻¹, respectively, due to increased extreme rains in the Mississippi/Atchafalaya river basin, and this intensification of erosional N and P fluxes drive the significant increase of riverine PN and PP yields to the northern Gulf of Mexico. With extreme rains projected to increase with warming, erosional nutrient fluxes in the region would likely continue to rise in the future, thus complicating the effort of reducing eutrophication in the inland and coastal waters.

1. Introduction

Soil erosion is one of the most important pathways for the lateral fluxes of nitrogen (N) and phosphorus (P) from land to rivers (Pimentel and Kounang 1998, Beusen *et al* 2005, Liu *et al* 2010, Berhe *et al* 2018). Unlike soil leaching that dominates the lateral fluxes of dissolved N and P, erosional N and P fluxes are mostly in particulate forms and can contribute as much as 34% and 78% of riverine N and P yields to oceans, respectively, across the globe (Seitzinger *et al* 2010). With carbon (C) and nutrient cycling closely coupled in terrestrial and aquatic ecosystems

(Peñuelas *et al* 2013), this massive transfer of N and P has immense influences on the global and regional ecology and biogeochemistry (Ward *et al* 2017). On land, the loss of N and P would degrade soil quality and limit atmospheric CO₂ fixation by vegetations (particularly crops) (Berhe *et al* 2018). In surface waterbodies, erosional particulate N and P (hereafter referred to as PN and PP, respectively) gained from land can be remobilized in the water column through chemical transformations (e.g. desorption of inorganic N and P from reduced iron, manganese and other redox-sensitive compounds, and mineralization of organic N and P) (Sutula *et al* 2004, Ward *et al*

2017). These mobilized nutrients will then be easily accessible to aquatic organisms. Further, data showed that PP is frequently more abundant than dissolved forms of P in inland waters (Meybeck 1982, Froelich 1988, Goolsby *et al* 1999, Seitzinger *et al* 2010).

Recent surveys showed that excessive N and P loadings mainly from anthropogenic sources are responsible for high levels of N and P eutrophication in over a quarter of streams and one-fifth of lakes in the United States (US) (US EPA 2009, 2013) and for development of the world's second largest coastal hypoxic zone during summertime in the northern Gulf of Mexico (Rabalais *et al* 1999, Sylvan *et al* 2006, Dale *et al* 2007). Although the US government has invested billions of dollars in managing N and P inputs from anthropogenic sources (Jeppesen *et al* 2005, Mississippi River/Gulf of Mexico Watershed Nutrient Task Force 2015), the results are not always as good as expected (Finlay *et al* 2013, Van Meter *et al* 2018). These unsatisfactory outcomes could be partly attributed to the nutrient legacy effect, i.e. N and P that entered watersheds a long time ago continue to sustain soluble reactive N and P levels in inland and coastal waters through groundwater discharge, inorganic matter desorption and organic matter decomposition (Froelich 1988, Finlay *et al* 2013, Van Meter *et al* 2018, Kreiling *et al* 2019). As such, realistic estimates of erosional N and P fluxes are essential to understand and manage the N and P enrichment in the northern Gulf of Mexico and over the continental US.

Furthermore, erosional N and P fluxes (i.e. soil erosion driven PN and PP loads to inland waters) are tightly connected to both water and biogeochemical cycles. It is thus important to represent such processes in Earth system models to understand their evolution in the context of climate change (Gonzalez-Hidalgo *et al* 2010, Tan *et al* 2017) and their interactions with other environmental changes (Scavia *et al* 2002, Heisler *et al* 2008). For this purpose, we develop a new process-based model to represent erosional N and P fluxes within the framework of the E3SM (Golaz *et al* 2019, Burrows *et al* 2020). Upon successful validation of the model in the continental US, we use it for two scientific questions: (a) how may observed climate variability in recent decades impact erosional N and P fluxes in the continental US? (b) How may changes in erosional N and P fluxes influence eutrophication, defined as over-enrichment in bioavailable nutrients, in inland and coastal waters? Particularly, we focus on the Mississippi/Atchafalaya river basin (MARB) that has a strong influence on hypoxia and other environmental issues in the northern Gulf of Mexico.

2. Materials and methods

2.1. Model description

We develop a new erosional N and P model building on an existing soil erosion module within the E3SM land model (ELM) (hereafter referred to as

ELM-Erosion) (Tan *et al* 2020). ELM-Erosion is essentially an improved version of the Morgan–Morgan–Finney soil erosion model (Morgan 2001) and runs with a daily time step (Tan *et al* 2018). It simulates soil erosion and erosion-induced lateral fluxes of sediment and particulate organic carbon (POC) based on ELM simulated hydrological, ecological and biogeochemical conditions (Tan *et al* 2020). We validated ELM-Erosion at small catchment scales (Tan *et al* 2018), and further demonstrated its ability to capture the spatial variability of soil erosion and sediment and POC yield in large river basins of the continental US, including the MARB and its sub-basins (Tan *et al* 2020). The effectiveness of ELM in simulating the spatial and temporal variability of land hydrology and soil C, N and P pools have been well documented in previous studies (Ricciuto *et al* 2018, Golaz *et al* 2019, Zhu *et al* 2019, Burrows *et al* 2020).

In this work, we extend ELM-Erosion to include erosional N and P fluxes defined as the product of erosional POC flux and soil particle C/N and C/P mass ratios in surface soils. ELM has two representations of soil biogeochemistry based on the Equilibrium Chemistry Approximation (ECA) and Convergent Trophic Cascade (CTC) routines (Burrows *et al* 2020). Soil C, N and P cycle among different forms (i.e. organic and inorganic forms), with inputs from litterfall, fertilization and atmospheric deposition, and outputs through decomposition, plant uptake, nitrification/denitrification, erosion and runoff/leaching (Yang *et al* 2014, Zhu *et al* 2016). Specifically, the particulate forms of soil C, N and P in ELM are represented by three soil organic matter pools with different turnover times in the ECA routine versus four soil organic matter pools with different turnover times in the CTC routine (Yang *et al* 2014, Zhu *et al* 2016). In addition, both routines represent the particulate forms of soil P with four mineral pools (inorganic labile P, parent material P, secondary mineral P and occluded P) (Yang *et al* 2014, Zhu *et al* 2016). Correspondingly, the ELM-Erosion model assumes that erosional PN originates dominantly from soil organic N pools, whilst erosional PP originates from both soil organic P pools and mineral P pools, which is also consistent with Berhe *et al* (2018).

In this study, instead of relying on a single soil biogeochemistry routine, we use an ensemble approach to estimate erosional PN and PP fluxes. Using an ensemble approach is important because (a) soil particle C/N and C/P ratios simulated by soil biogeochemistry routines usually have large uncertainties (supplementary figure S1 (available online at stacks.iop.org/ERL/16/054080/mmedia)), (b) soil biogeochemistry routines usually do not well resolve the vertical variation of C:N:P stoichiometry in the soil column (Rostad *et al* 1997, Tipping *et al* 2016), and (c) the C/N and C/P ratios in eroded soils are usually much lower than those in surface soils due

to the preferential erosion of N- and P-rich fine soil particles (Meybeck 1982, Lindström *et al* 2010). In the ensemble approach, the C/N and C/P ratios in eroded soils are estimated using three methods: the CTC routine, the ECA routine and the empirical method of Beusen *et al* (2005). The empirical equations of the C/N and C/P ratios in Beusen *et al* (2005) were compiled from a large observational dataset of riverine N and P:

$$\text{PN}_c = 0.116\text{POC}_c - 0.019, \quad (1)$$

$$\text{PP}_m = \frac{\text{POC}_m^{1.002}}{22.1536}, \quad (2)$$

where PN_c and POC_c are the contents of PN and POC in percentage in eroded soils, respectively, and PP_m and POC_m are the mass fluxes (kg yr^{-1}) of eroded PP and POC. POC_c is calculated as the ratio of soil organic C density to soil bulk density. Noticeably, because the exponent of POC_m is close to 1, the C/P ratio calculated from equation (2) is mostly at a constant value of 22 for rivers worldwide. This C/P ratio of 22:1 is consistent with the reported value of Meybeck (1982).

The change of soil N and P pools after erosion are modeled in ELM-Erosion following the method of Naipal *et al* (2018). In this method, the loss of C, N and P by erosion from the surface soil layer causes the vertical displacements of C, N and P from the deeper soil layers. At the bottom of the soil column, where no soil layer exists underneath, we assume that only parent material P can be moved upward from the bottom.

Because E3SM does not yet represent river biogeochemistry, we cannot directly estimate how much PN and PP are lost in river systems during transport through either deposition or degradation. Instead, we estimate riverine PN and PP yields from river basins based on the nutrient spiraling theory of inland waters which assumes that the nutrient retention in rivers is an exponential function of the travel time of nutrient molecules in the river network (Runkel 2007):

$$\text{PN}_o = \sum \text{PN}_i e^{-\lambda_{\text{PN}}\tau_i}, \quad (3)$$

$$\text{PP}_o = \sum \text{PP}_i e^{-\lambda_{\text{PP}}\tau_i}, \quad (4)$$

where PN_i and PP_i are erosional PN and PP fluxes from a grid cell in a river basin (kg yr^{-1}), respectively, PN_o and PP_o are erosional PN and PP yields from the river basin (kg yr^{-1}), respectively, τ_i is the water residence time for a grid cell in the river basin (yr), λ_{PN} and λ_{PP} are PN and PP retention rates in the channels of the river basin (yr^{-1}), respectively. In E3SM, the river water resident time is estimated by the Model for Scale Adaptive River Transport (MOSART)

river model which simulates runoff routing using the kinematic wave method, considering channel geometry and roughness (Li *et al* 2013). MOSART has been coupled with a water management model that represents reservoir operation and irrigation and their impacts on streamflow (Voisin *et al* 2013). The basin-scale PN and PP retention rates λ_{PN} and λ_{PP} are calibrated by minimizing the difference between estimated and observed riverine PN and PP yields, respectively.

2.2. Simulation protocol

Following Tan *et al* (2020), numerical experiments are conducted over the North American Land Data Assimilation System (NLDAS) 1/8-th degree resolution latitude/longitude grid for the period of 1991–2019 driven by the NLDAS-2 atmospheric forcing data (Mitchell *et al* 2004). The ELM land biogeochemistry is first spun up for 200 years with accelerated decomposition spin-up and then another 600 years with regular spin-up, using repeated atmospheric forcing from an E3SM preindustrial simulation (Golaz *et al* 2019). More details about the ELM spin-up process are described in Burrows *et al* (2020). After the total ecosystem C has reached an equilibrium, the model is then run from 1850 to 1990 using atmospheric forcing from an E3SM historical simulation to generate initial conditions for the land states.

Cropland erosion management (e.g. no tillage) is a critical factor governing soil erosion over agricultural land (Montgomery 2007, Meade and Moody 2010). In theory, because the application of conservation practices affects the canopy cover and ground cover, these conservation practices should be directly parameterized in ELM-Erosion. However, as ELM-Erosion and Revised Universal Soil Loss Equation (RUSLE) have very different model structures and run on different spatial resolutions, it is difficult for ELM-Erosion to effectively parameterize conservation practices. For example, the support practice factor and prior-land-use factor used by RUSLE need high-resolution data of conservation measures and soil properties to calculate, which is difficult for the coarse resolution ELM. Further, conservation practices usually affect soil erosion in a combined manner, which means that simply implementing one or two RUSLE subfactors in ELM may not improve the model performance substantially. Thus, ELM-Erosion adopts a data-driven approach to mimic its effect. First, we extracted the state-level soil erosion intensity in cropland from the USDA National Resources Inventory (NRI) benchmark estimates (USDA 2018). The NRI estimates were based on the RUSLE approach which includes three dynamic factors (Renard *et al* 1997): the rainfall erosivity factor R , the cover-management factor C , and the support practice factor P . During our simulation period of 1991–2019, the effect of the R factor

on the erosion dynamics is minor because there is no discernible trend in mean annual rainfall (see our discussions below) and this factor is less sensitive to extreme rainfall when calculated based on coarse resolution precipitation data (Tan *et al* 2018). As such, the temporal variability of the estimated soil erosion intensity should mainly reflect the temporal variability of cropland management (the *C* and *P* factors). In the next step, we interpolated the 5 year interval NRI estimates linearly in time to construct annual erosion intensity time series at each grid cell during 1991–2019, which were then normalized by the erosion intensity of the grid cell in 1991 (supplementary figure S2). We then apply the normalized soil erosion intensity as an adjustment multiplier to the equations of rainfall- and runoff-driven erosion (Tan *et al* 2020 and supplementary text S1) to account for the change in crop management effect relative to 1991.

We conducted three ensembles of simulations in this study, with each ensemble corresponding to one scenario. The first scenario S0 uses the adjustment factor for cropland erosion management described above. The second scenario S1 does not use the adjustment factor. The third scenario S2 is similar to S0 except that the rainfall forcing is manipulated. Each ensemble consists of three simulations with the C/N and C/P ratios in eroded soils estimated using the CTC routine, the ECA routine and the empirical method. Between S0 and S1, another difference is that S0 includes the change of land use based on the Land Use Harmonized version 2 transient dataset (Hurt *et al* 2011, supplementary figure S3) but S1 does not. Because our study focuses on the erosional loss of PN and PP in soils while N and P sourced from fertilizer and manure applications are mostly lost through runoff and leaching (Berhe *et al* 2018), we do not expect fertilizer and manure applications to affect our simulations significantly. However, as nutrient limitation is important for plant growth, we apply N fertilization in the S0 and S1 simulations to better quantify the impact of plant canopy cover and ground cover on erosion. In ELM, N fertilization is applied to the crop land units based on prescribed crop-specific fertilization rates (Oleson *et al* 2013). P fertilization is not considered in our study because it has not been implemented in ELM (Oleson *et al* 2013), and it is perceived to mainly impact plant growth in tropical regions (Zhu *et al* 2019). Model validation is based on S0 which is a more realistic configuration accounting for land use change and temporal variations in crop management effect, but analysis of how climate impacts erosional nutrient fluxes is based on the climate-only scenario S1.

The rainfall manipulation scenario S2 was conducted to isolate the effect of extreme rains on erosional PN and PP fluxes. The major difference between S2 and S0 is that the interannual variations of non-extreme rainfall in the NLDAS-2 atmospheric

forcing data are removed for S2. Specifically, for each year of 1991–2019, we first divide all the days in each grid cell into two groups: the days with extreme rains and the days without extreme rains. Days with extreme rains are determined by the 95th percentile of all daily rains of the year. We then repeat the rainfall data of 1991 for 28 years to construct the rainfall data of 1992–2019. Finally, we replace the extreme rainfall in the constructed rainfall data for each year of 1992–2019 with the extreme rainfall from the real rainfall data of 1992–2019.

2.3. Model validation and statistical analysis

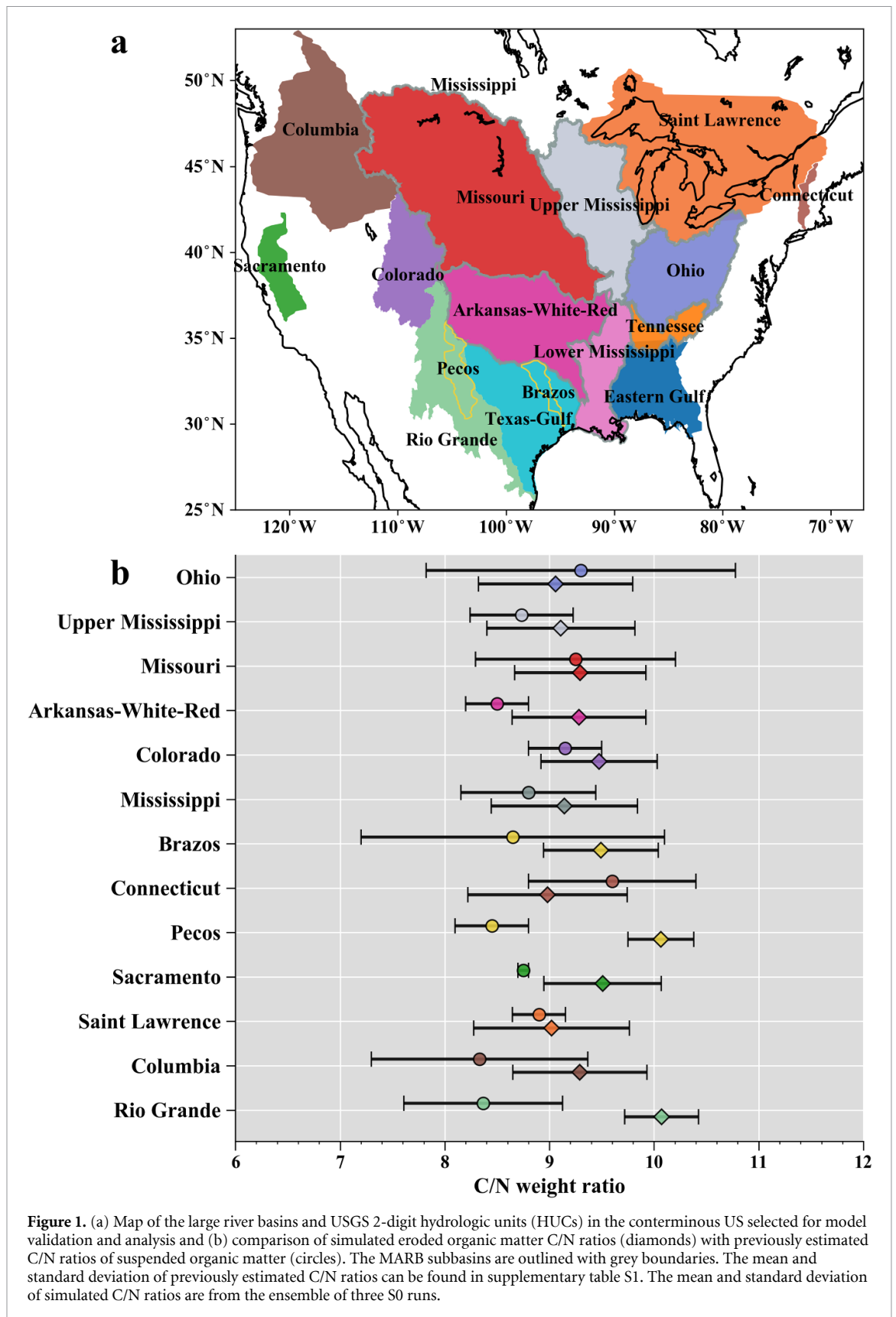
To validate the simulated C/N and C/P ratios of detached sediment that enters rivers, we collected published C/N and C/P ratios of suspended sediment for selected large US rivers (figure 1(a)) from a literature review (supplementary table S1). Noticeably, due to biogeochemical processes, the C/N and C/P ratios of suspended sediment can vary during transport, which might introduce uncertainties to the validation. To validate the dynamics of estimated riverine PP flux, we used the observed riverine PP (total P minus orthophosphate) yield data for the MARB and its sub-basins from USGS (Lee and Reutter 2019). Our validation focuses on the temporal variability of riverine PP flux but not PN flux because we do not have observed PN flux for such a comparison. Noticeably, using a similar method (total N minus dissolved N) to estimate riverine PN flux from the USGS total and dissolved N data is not appropriate. It is because terrestrial PN only contributes to a small fraction of total riverine N (Meybeck 1982, Goolsby *et al* 2000), and dissolved N in rivers is strongly controlled by N fixation, nitrification and denitrification. Model performance is assessed using three metrics: relative error, the coefficient of determination (R^2) and Nash–Sutcliffe coefficient.

Here for each grid cell, we define extreme rains as daily rainfall that is above the 95th percentile of all daily rains during 1991–2019. Correspondingly, the surface runoff and erosional N and P fluxes during the days with extreme rains are marked as extreme rainfall driven. For both hydrological and nutrient fluxes, their trends of annual total and extremes are calculated using linear regressions and verified by the Mann–Kendall test with the significant value of 0.05.

3. Results and discussion

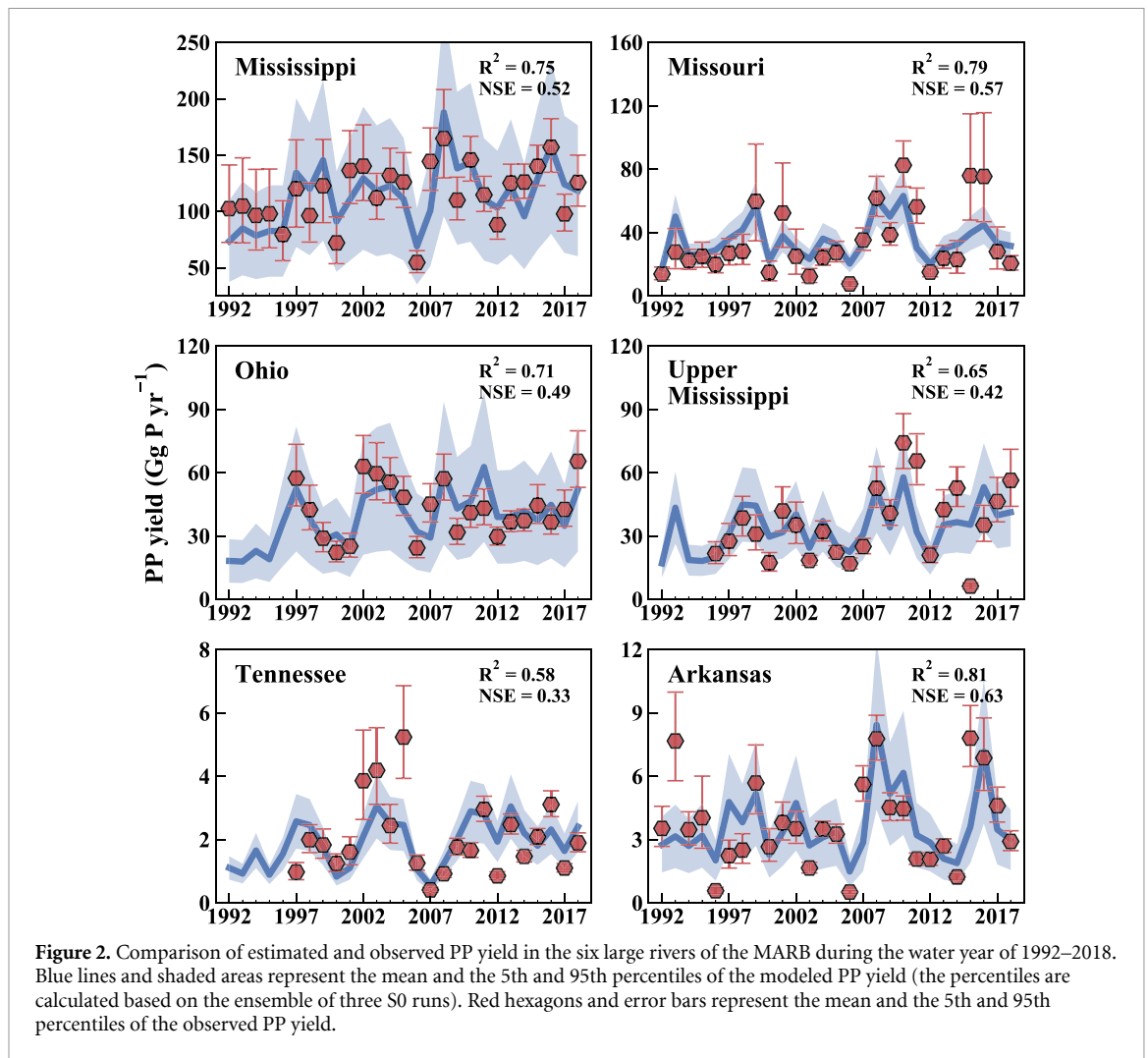
3.1. Model validation

Model validation shows that ELM-Erosion can reproduce the C/N ratios of suspended sediment in the large rivers of the continental US (figure 1). Because ELM-Erosion already captures the spatial variability of POC fluxes in the continental US (Tan *et al* 2020, supplementary figure S4), the realistic simulation of C/N ratios means that the model can also reproduce the spatial variability of erosional N flux. In fact, in



most cases (even including the Arkansas, Sacramento and Rio Grande rivers), the estimated C/N ratios from equation (1) have relative errors less than 10%. Noticeably, the rivers with large positive model biases of C/N ratios are all in the regions of warm climate,

suggesting that the positive biases could partly be caused by in-river biogeochemical processes, such as primary production, which are not represented in E3SM. As illustrated, the simulated C/P ratios of suspended sediment by equation (2) are very close



to 22 across the continental US, which is consistent with observations documented by Meybeck (1982). Encouragingly, the interannual variability of estimated riverine PP yield is consistent with observations in the large rivers of the MARB (figure 2). In some cases, our method fails to capture the extreme high or low PP yield in the observations, such as the observed extremes of PP yields in the Missouri and Tennessee rivers (figure 2), which could be caused by the oversimplification of river PP retention in our method. For example, river PP deposition may deviate from the normal condition during extremely wet and dry years. Both model estimates and observations show that the riverine PP yield in the MARB increases during the water year of 1992–2018: the observed trend is 1.3 Gg P yr^{-1} ($1 \text{ Gg} = 1 \times 10^9 \text{ g}$) (Mann–Kendall test, $p < 0.05$) and the estimated trend is 1.7 Gg P yr^{-1} (Mann–Kendall test, $p < 0.05$). Here a water year is defined as the 12 month period starting from October 1 prior to a given year. Due to in-river deposition and biogeochemistry, only a small fraction of erosional PP flux eventually reaches river outlets (supplementary table S2): on average $38 \pm 5\%$ in the MARB.

Results from simulations S0 show that soil erosion can drive enormous amounts of PN and

PP transferring from land to inland waters in the continental US during 1991–2019. On average, soil erosion delivered about $1047 \pm 269 \text{ Gg N}$ of PN and $445 \pm 215 \text{ Gg P}$ of PP, respectively, to rivers each year (figure 3). In the continental US, the MARB contributed the largest erosional N and P fluxes: about $718 \pm 102 \text{ Gg N yr}^{-1}$ and $302 \pm 105 \text{ Gg P yr}^{-1}$, respectively. Within the MARB, most of the erosional N and P fluxes originate from the Missouri, Ohio and Upper Mississippi river basins (Goolsby *et al* 1999, 2000, Goolsby and Battaglin 2001) because of their vast cropland areas (Tan *et al* 2020, figure 3). Noticeably, as more than 60% of eroded soils are redeposited on land and never entered the river networks in the region (Tan *et al* 2020), the amounts of soil N and P disturbed by erosion are much larger than the amounts of erosional PN and PP loads to rivers (figure 3 and supplementary figure S5). Thus, the impact of soil erosion on soil N and P cycling is likely much larger than what we presented here.

The modeled erosional N and P fluxes cannot be directly compared with riverine PN and PP yields, because of retention of PN and PP in river networks by reservoir trapping and chemical transformations (Maavara *et al* 2020). However, the modeled erosional

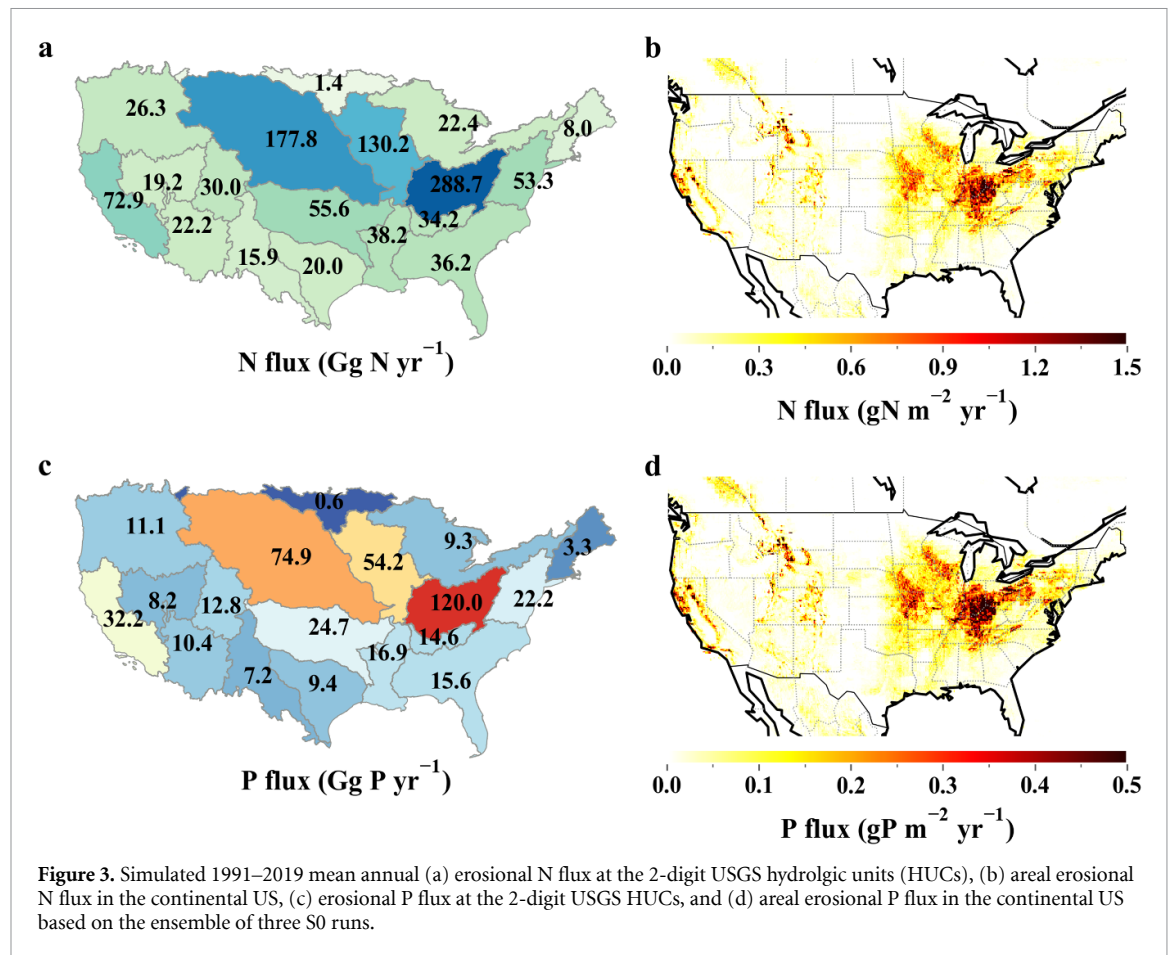


Figure 3. Simulated 1991–2019 mean annual (a) erosional N flux at the 2-digit USGS hydrologic units (HUCs), (b) areal erosional N flux in the continental US, (c) erosional P flux at the 2-digit USGS HUCs, and (d) areal erosional P flux in the continental US based on the ensemble of three S0 runs.

N and P fluxes are expected to be within the bounds of the measured riverine post-dam PN and PP yields (the lower bound) and pre-dam PN and PP yields (the upper bound). Using gauge data, Goolsby and Battaglin (2001) estimated the mean annual post-dam PN yield from the MARB during 1980–1996 to be about 210 Gg N yr⁻¹. Meanwhile, the pre-dam PN yield from the MARB is about 600 Gg N yr⁻¹, which is based on the assumption of 0.15% N content in suspended sediment (Goolsby *et al* 2000) and 4×10^5 Gg of suspended sediment yield in the pre-dam condition (Milliman and Syvitski 1992). Our modeled erosional N flux of 718 ± 102 Gg yr⁻¹ in the MARB is at the higher end of the above range. It is also larger than the modeled mean annual PN flux from the MARB (320 ± 160 Gg N yr⁻¹) estimated by Beusen *et al* (2005). A possible reason for our higher estimate is that soil C and N contents simulated by the ELM soil biogeochemistry are higher than the prescribed values of Goolsby *et al* (2000) and Beusen *et al* (2005). Another possible reason is that as shown in our study, the erosional N flux has continued increasing since 2000s. Our estimate of PN flux from the Saint Lawrence river basin (31 ± 7 Gg N yr⁻¹) is of the same order of magnitude as the river measurements (22–42 Gg N yr⁻¹) during 1981–1985 (Pocklington and Tan 1987). For the MARB, our modeled erosional P flux is within the range of the observed post-dam

riverine PP yield (on average 95 Gg P yr⁻¹ during 1980–1996) (Goolsby *et al* 1999) and the estimated pre-dam riverine PP yield (about 415 Gg P yr⁻¹) (Meybeck 1982, Milliman and Syvitski 1992).

3.2. Impacts of climate and land management changes

The impact of cropland erosion management on erosional N and P fluxes during 1991–2019 is moderate. Compared with S0, erosional N and P fluxes in the continental US in S1 (ignoring cropland erosion management and land use change) are only about 76 Gg N and 32 Gg P higher, respectively, on average (table 1). Similarly, compared with S0, erosional N and P fluxes from the MARB in S1 are only about 70 Gg N and 29 Gg P higher, respectively, on average (table 1). The small difference in erosional N and P fluxes between simulations S0 and S1 can be explained by (a) the gradual maturity of cropland erosion management methods since 1990s that slowed down erosion reduction (supplementary figure S2) and (b) the small fraction of eroded soils that can enter the river networks due to limited sediment transport capability by surface runoff (Tan *et al* 2020). However, without including cropland erosion management and land use change, erosional N and P fluxes would have increased more quickly in the continental US (particularly in the MARB)

Table 1. Summary of the simulation results of the three scenarios S0–S2.

	Units	S0	S1	S2
Erosional N flux in the continental US	Gg N yr ⁻¹	1047 ± 269	1123 ± 293	856 ± 215
Erosional P flux in the continental US	Gg P yr ⁻¹	445 ± 215	477 ± 206	364 ± 206
Erosional N flux in the MARB	Gg N yr ⁻¹	718 ± 102	788 ± 112	583 ± 81
Erosional P flux in the MARB	Gg P yr ⁻¹	302 ± 105	331 ± 109	246 ± 102
Erosional N flux in the drainage basins of the northern Gulf of Mexico	Gg N yr ⁻¹	775 ± 108	848 ± 119	636 ± 87
Erosional P flux in the drainage basins of the northern Gulf of Mexico	Gg P yr ⁻¹	328 ± 110	359 ± 114	270 ± 108
Mean trend of erosional N flux in the MARB	Gg N yr ⁻¹	14.6	19.8	10.6
Mean trend of erosional P flux in the MARB	Gg P yr ⁻¹	6.1	8.2	4.4
Mean trend of erosional N flux in the drainage basins of the northern Gulf of Mexico	Gg N yr ⁻¹	14.8	20.2	11.2
Mean trend of erosional P flux in the drainage basins of the northern Gulf of Mexico	Gg P yr ⁻¹	6.2	8.4	4.6

during 1991–2019. For example, the increasing trend of erosional P flux in the MARB in S1 is 8.2 Gg P yr⁻¹ (Mann–Kendall test, $p < 0.05$), which is 2.1 Gg P yr⁻¹ (34%) higher than that in S0 (table 1).

Based on the ensemble of three S0 runs, we estimate that soil erosion generates 775 Gg yr⁻¹ of PN flux and 328 Gg yr⁻¹ of PP flux on average to the drainage basins of the northern Gulf of Mexico during 1991–2019 (table 1). Since the MARB is the largest source of PN and PP for the northern Gulf of Mexico (on average 93% and 92%, respectively), increases in erosional N and P fluxes from the MARB drove significant positive trends (Mann–Kendall test, $p < 0.05$) of erosional N and P fluxes from land to the drainage basins of the northern Gulf of Mexico (figure 4): about 15 Gg N yr⁻¹ and 6 Gg P yr⁻¹, respectively during 1991–2019 (table 1). Far behind the MARB, the Texas-Gulf region (supplementary figure S4) is ranked second in contributing erosional N and P fluxes to the northern Gulf of Mexico: on average 3% of N and 3% of P, respectively. As indicated by the riverine N and P data in the MARB, the fraction of PN in the total riverine N is only 30%, but the fraction of PP in the total riverine P is as large as 70% (Goolsby *et al* 2000, Goolsby and Battaglin 2001, Lee and Reutter 2019). The relative contributions of dissolved and PN and PP to the total riverine N and P are probably determined by the difference in land N and P export pathways (i.e. leaching, runoff and soil erosion) rather than in-stream processes (supplementary figures S7–S8). As such, it is reasonable to conclude that the increase of erosional nutrient flux should have a much more significant impact on P enrichment than N enrichment in the northern Gulf of Mexico. Moreover, erosional PP in the region consists of a large fraction of organic and inorganic P that are bioavailable to aquatic organisms (supplementary figure S8). Over 55% of eroded P consists of soil organic P and mineral P that can be degraded or desorbed within decades (active and slow soil organic matter, labile PP and secondary mineral

PP), hence contributing to the nutrient legacy effect. Because P is an important limiting nutrient for algal growth during spring and early summer in the northern Gulf of Mexico (Sylvan *et al* 2006, Dale *et al* 2007), the increase of erosional P flux may enhance P enrichment and exacerbate other environmental issues in the coastal waters (Cai *et al* 2011, Laurent and Fennel 2017).

Without considering cropland erosion management and land use change, erosional N and P fluxes to the drainage basins of the northern Gulf of Mexico could have increased at faster rates (Mann–Kendall test, $p < 0.05$) of 20.2 Gg N yr⁻¹ and 8.4 Gg P yr⁻¹, respectively during 1991–2019 (table 1). Soil erosion in ELM-Erosion is jointly controlled by the change of climate and vegetation cover (supplementary text S1). As the change of vegetation cover only plays a minor role in soil erosion evolution during the period (Tan *et al* 2020), the positive trends of erosional N and P fluxes are thus mostly caused by the change of rainfall and runoff. Furthermore, as shown in figure 5(a), the increase of rainfall and runoff mainly occurs in the Ohio, Tennessee and Upper Mississippi river basins. Noticeably, erosional N and P fluxes share similar spatio-temporal variabilities because they are both dominated by the variability of sediment flux instead of that of soil PN and PP pools (Berhe *et al* 2018). We differentiate the simulated erosional P flux into two groups: those occurring on days with extreme rain events, and those occurring on days without extreme rain events. We find that as much as 80% of the positive trend of erosional P flux in the three river basins is dominated by the increase of erosional P flux in the first group (figures 5(b)–(d)). The weaker P flux trend in the second group is due to the negligible increase of mean annual rainfall and runoff (figures 5(e) and (f)). Further analysis shows that the total extreme rainfall volume per year actually only increases mildly during 1991–2019 (figure 5(g)). However, due to the nonlinear relationship between rain intensity and

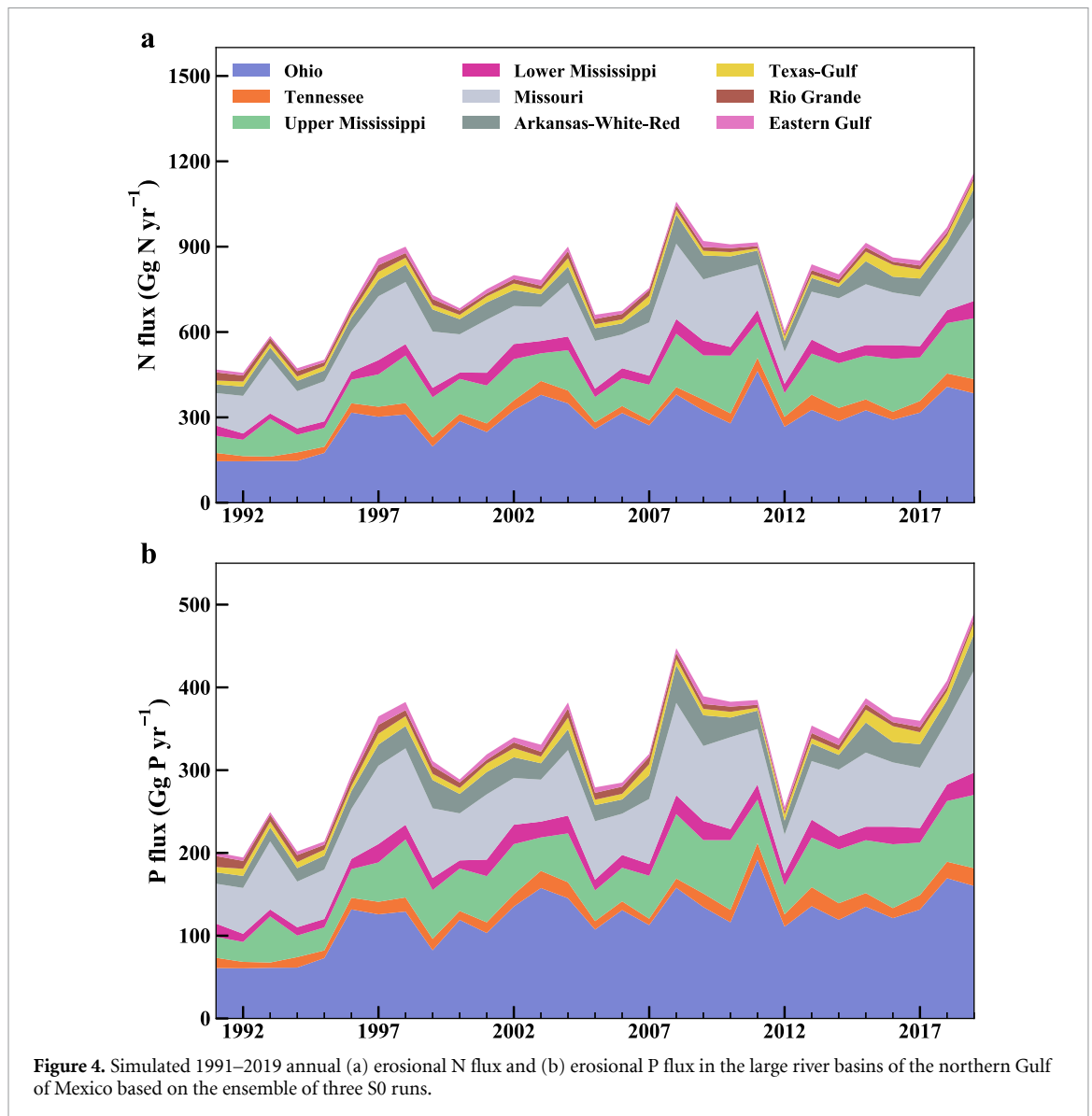


Figure 4. Simulated 1991–2019 annual (a) erosional N flux and (b) erosional P flux in the large river basins of the northern Gulf of Mexico based on the ensemble of three S0 runs.

runoff generation (Gonzalez-Hidalgo *et al* 2010), the mild increase of extreme rains causes a much larger increase of surface runoff extremes (figure 5(h)).

As documented in our observation-based analysis, soil erosion is highly responsive to rain and runoff extremes (Tan *et al* 2017). Hence, the increase of extreme rainfall and runoff in the three river basins drives significant increases of erosional N and P fluxes to the northern Gulf of Mexico. With the same river retention ratios as simulations S0 but allowing only extreme rains to vary temporally while interannual variability of non-extreme rains is removed, simulations S2 shows a similar increase of riverine PP yield in the MARB in recent decades (supplementary figure S9): 2.3 Gg P yr^{-1} (Mann–Kendall test, $p < 0.05$). Hence the rainfall manipulation test S2 provides further support of the role of extreme rains in the increased erosional N and P fluxes in recent decades. Furthermore, we compared the histograms of simulated erosional P fluxes at the two time periods of 1991–1995 and 2015–2019 to highlight the trend

(figure 4). Consistently, this analysis also suggests that large erosional P production occurs more frequently during 2015–2019 than during 1991–1995 in the three river basins (figure 6). Particularly in the Ohio river basin, daily erosional P flux larger than $9 \text{ mg P m}^{-2} \text{ d}^{-1}$ was absent during 1991–1995 but starts emerging during 2015–2019.

4. Limitations and future development

Previous studies showed that sediment yields in the MARB and many of its sub-basins have been decreasing in recent decades due to reduction of soil erosion and increase of sediment trapping in reservoirs (Meade and Moody 2010, Mize *et al* 2018, Murphy 2020). There are two possible explanations for the contradicting trends between the observed sediment and PP yields in the MARB. First, despite the reduction of soil erosion, the increase of overland sediment transport (supplementary figure S10) may actually have increased sediment loads to rivers

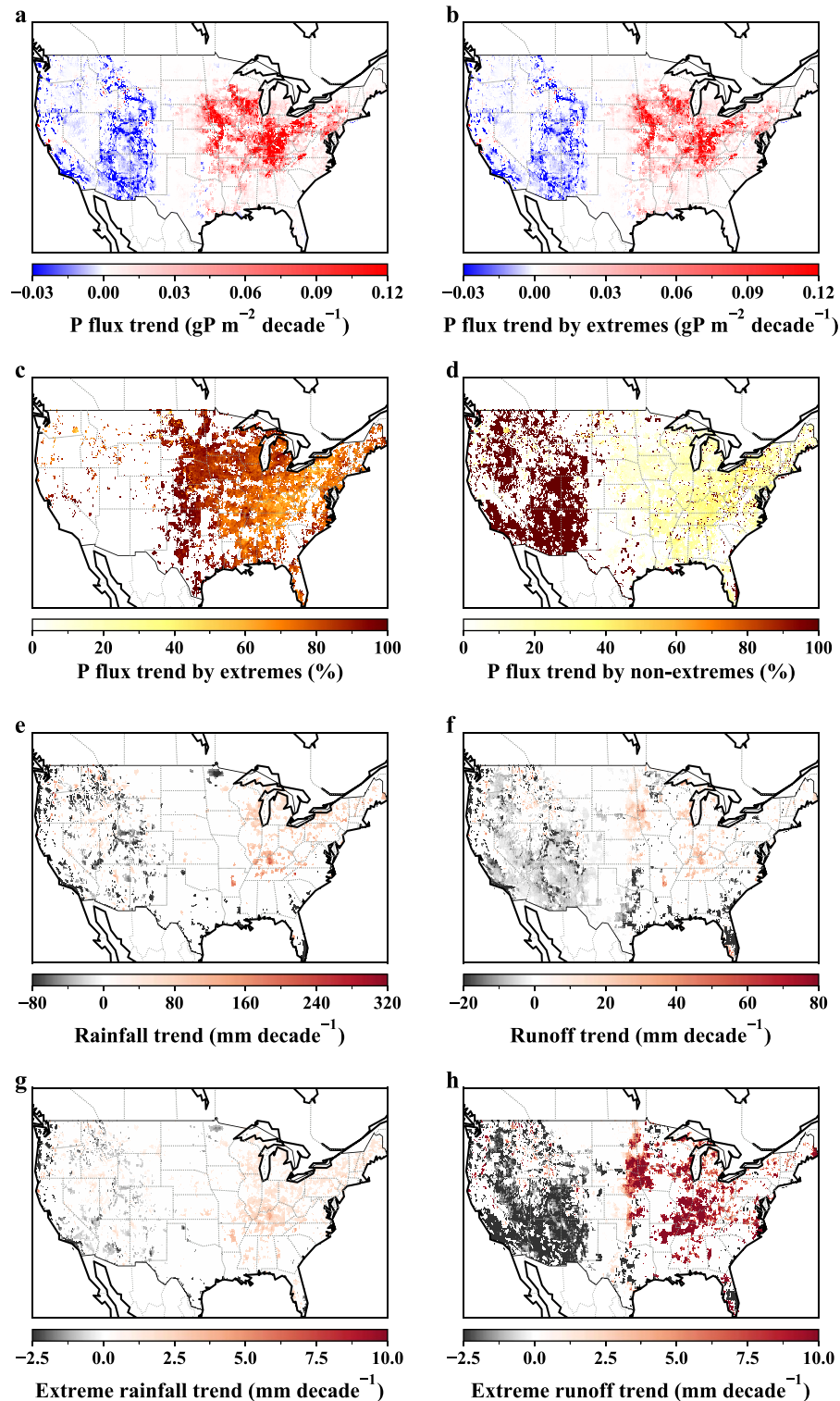


Figure 5. Simulated (a) decadal trend of erosional P flux, (b) decadal trend of erosional P flux associated with 95th percentile daily rain extremes, (c) the percentage of decadal erosional P flux trend associated with rain extremes, (d) the percentage of decadal erosional P flux trend associated with non-extreme rains, (e) decadal trend of annual rainfall, (f) decadal trend of annual surface runoff, (g) decadal trend of annual rainfall associated with 95th percentile daily rain extremes, and (h) decadal trend of annual surface runoff associated with 95th percentile daily rain extremes during the period of 1991–2019. In (a)–(h), colors are only drawn on grid cells with significant trends (Mann–Kendall test, $p < 0.05$). In (c) and (d), negative trend is not shown. (a)–(d) are based on the ensemble of S1 runs.

in recent decades. However, because sediment yield in the MARB was strongly regulated by the river sediment budget which has been decreasing in recent decades (Meade and Moody 2010), the increase in

sediment loads was not potent enough to increase the sediment yield. Second, despite the reduction of total sediment loads, loads of fine sediments that contain more PP may actually have increased. Notably, the

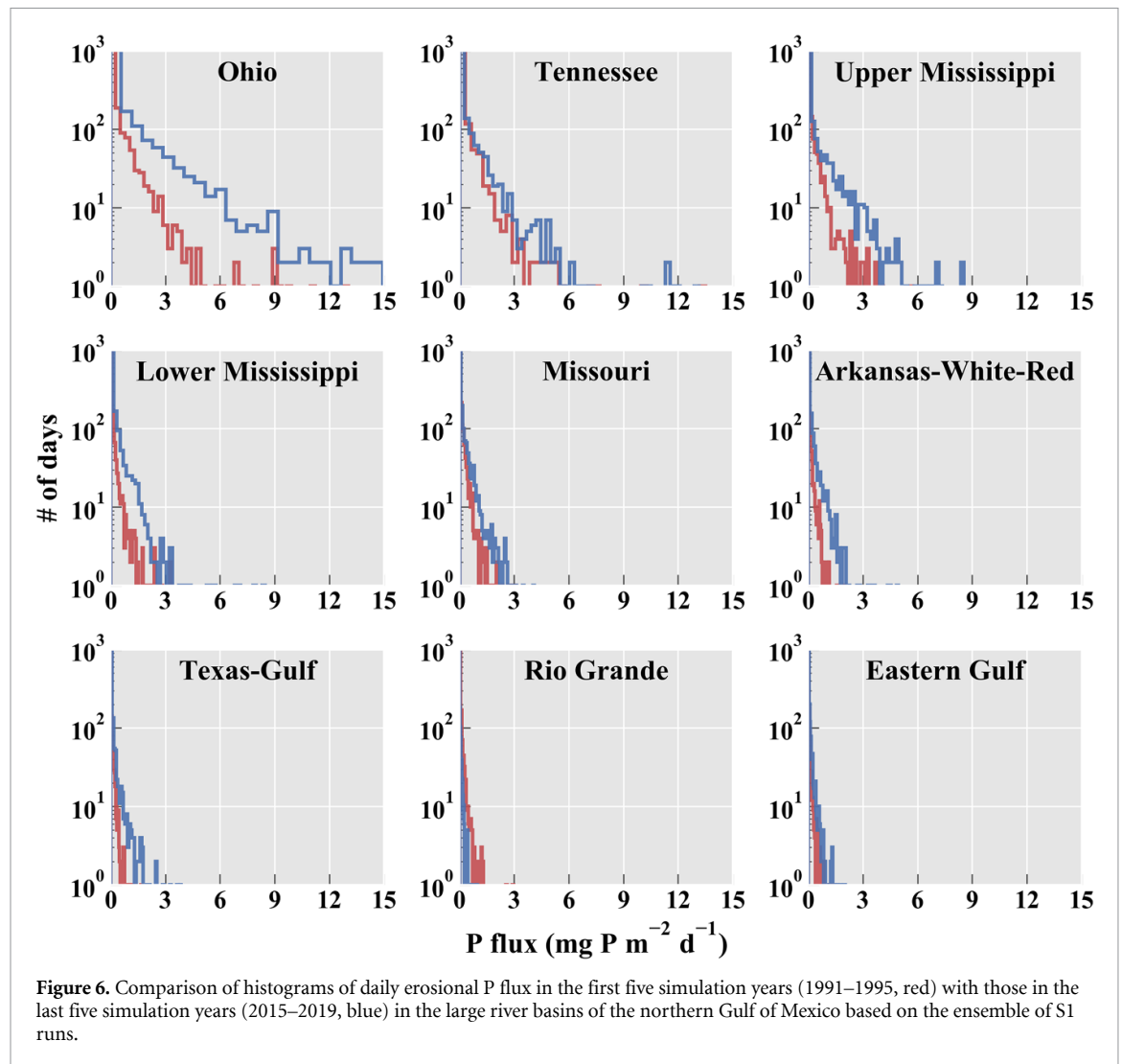


Figure 6. Comparison of histograms of daily erosional P flux in the first five simulation years (1991–1995, red) with those in the last five simulation years (2015–2019, blue) in the large river basins of the northern Gulf of Mexico based on the ensemble of S1 runs.

observations also confirm the increase of sediment yield in the Ohio river basin during 1991–2012 (Murphy 2020) where our estimated PP yield trend is the strongest (figure 4). But we acknowledge that the possibility of the second explanation cannot be fully excluded by our results because our model does not represent management actions (such as the use of riparian buffer strips) to attenuate sediment loads to rivers.

Our findings that erosional N and P fluxes are enhanced significantly in the MARB by the increase of extreme rainfall events have two important implications. First, because extreme rains are projected to further increase in general under climate warming and the increase in extreme rains will be larger than the increase of mean annual rainfall (Allen and Ingram 2002, Du *et al* 2019), both the total amount and mean concentration of riverine PN and PP may further increase. As such, the impact of soil erosion on N and P enrichment in the northern Gulf of Mexico is expected to become larger in the future. Further, because soil erosion is the dominant pathway for riverine P loading, the increase of erosional flux will

influence P enrichment more substantially. Second, the mechanism described above could also affect other hazardous materials (e.g. heavy metals) that can be detached by erosion and transported to the MARB and the northern Gulf of Mexico (Presley *et al* 1980). Therefore, we suspect that fluxes of these hazardous materials could also increase in the future.

We note that a few limitations in the model may introduce large uncertainties in our simulations. These include the lack of representation of river nutrient retention, cropland erosion management, riparian management, and the interactive effect of climate and land use. For example, river retention of PN and PP is essential to determine their fluxes to coastal waters but related to complex physical and biogeochemical processes that cannot be fully represented by a single basin-scale retention rate. Practices of cropland and riparian managements for soil erosion and sediment loads can alter the response of erosional PN and PP fluxes to climate. Thus, the prediction of PN and PP loads to rivers must include the spatiotemporal evolution of these practices. Also, as climate and land use changes are interdependent,

it is important to study their interactive effect on erosional N and P fluxes. Our future work will prioritize the representation of PN and PP transformations in the biogeochemistry component of the E3SM river model (Li *et al* 2013). These processes have already been included in a few river biogeochemical models and are shown to influence fluxes of bioavailable nutrients and phytoplankton growth in the water column significantly (Minaudo *et al* 2018, Vilmin *et al* 2020). We also intend to include a realistic representation of cropland erosion management in ELM-Erosion, such as the management of plant residues (Smets *et al* 2008), to improve understanding of land–river–ocean interactions in regions outside of the continental US.

5. Conclusion

This study presents a new erosional N and P model building on an existing continuous soil erosion module within ELM. The model is validated for the large rivers in the continental US. Using the model, we estimate that during 1991–2019 soil erosion yields 775 Gg yr⁻¹ of PN and 328 Gg yr⁻¹ of PP on average to the MARB and other rivers draining to the northern Gulf of Mexico. In particular, the MARB sub-basins such as the Ohio, Missouri and Upper Mississippi river basins that have intense agricultural activities contribute the most of these lateral PN and PP fluxes. We find that due to intensified extreme rains in the MARB erosional N and P fluxes in the drainage basins of the northern Gulf of Mexico increase at significant rates of 15 Gg N yr⁻¹ and 6 Gg P yr⁻¹ during 1991–2019. Based on the nutrient spiraling model with the simulated river water residence time from MOSART, we indicate that the intensification of erosional N and P fluxes has driven the significant increase of riverine PN and PP yields to the northern Gulf of Mexico in recent decades. Because extreme rains are projected to rise with warming and the majority of erosional P comes from bioavailable soil P pools, erosional nutrient fluxes in the region would likely continue to rise in the future and contribute more to riverine/estuarine nutrient enrichment. Therefore, it is important to enhance soil erosion control measures (e.g. reduced tillage, cover management and riparian buffer strips) to reduce the transport of P and N to the northern Gulf of Mexico.

Data availability statement

All data that support the findings of this study are included within the article (and any supplementary files).


Acknowledgments

The authors thank the anonymous reviewers for their constructive comments. This research is supported

by the Office of Science of the US Department of Energy as part of the Earth System Modeling program through the Energy Exascale Earth System Model (E3SM) project. The Pacific Northwest National Laboratory is operated by Battelle for the US Department of Energy under Contract DE-AC05-76RLO1830. The source code of ELM-Erosion is publicly available through the E3SM GitHub repository (<https://github.com/E3SM-Project/E3SM>).

ORCID iDs

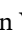
Zeli Tan  <https://orcid.org/0000-0001-5958-2584>

L Ruby Leung  <https://orcid.org/0000-0002-3221-9467>

Hong-Yi Li  <https://orcid.org/0000-0002-9807-3851>

Teklu Tesfa  <https://orcid.org/0000-0001-9267-4288>

Qing Zhu  <https://orcid.org/0000-0003-2441-944X>

Xiaojuan Yang  <https://orcid.org/0000-0002-2686-745X>

Maoyi Huang  <https://orcid.org/0000-0001-9154-9485>

References

- Allen M R and Ingram W J 2002 Constraints on the future changes in climate and the hydrological cycle *Nature* **419** 224–32
- Berhe A A, Barnes R T, Six J and Marín-Spiotta E 2018 Role of soil erosion in biogeochemical cycling of essential elements: carbon, nitrogen, and phosphorus *Annu. Rev. Earth Planet. Sci.* **46** 521–48
- Beusen A H W, Dekkers A L M, Bouwman A F, Ludwig W and Harrison J 2005 Estimation of global river transport of sediments and associated particulate C, N, and P *Glob. Biogeochem. Cycles* **19** GB4S05
- Burrows S M *et al* 2020 The DOE E3SM v1.1 biogeochemistry configuration: description and simulated ecosystem-climate responses to historical changes in forcing *J. Adv. Model. Earth Sys.* **12** e2019MS001766
- Cai W J *et al* 2011 Acidification of subsurface coastal waters enhanced by eutrophication *Nat. Geosci.* **4** 766–70
- Dale V *et al* 2007 *Hypoxia in the Northern Gulf of Mexico, an Update by the EPA Science Advisory Board; EPA-SAB-08-003* (Washington, DC: EPA Science Advisory Board)
- Du H *et al* 2019 Precipitation from persistent extremes is increasing in most regions and globally *Geophys. Res. Lett.* **46** 6041–9
- Finlay J C, Small G E and Sterner R W 2013 Human influences on nitrogen removal in lakes *Science* **342** 247–50
- Froelich P N 1988 Kinetic control of dissolved phosphate in natural rivers and estuaries: a primer on the phosphate buffer mechanism *Limnol. Oceanogr.* **33** 649–68
- Golaz J C *et al* 2019 The DOE E3SM coupled model version 1: overview and evaluation at standard resolution *J. Adv. Model. Earth Sys.* **11** 2089–129
- Gonzalez-Hidalgo J C, Batalla R J, Cerda A and de Luis M 2010 Contribution of the largest events to suspended sediment transport across the USA *Land Degrad. Dev.* **21** 83–91
- Goolsby D A and Battaglin W A 2001 Long-term changes in concentrations and flux of nitrogen in the Mississippi River Basin, USA *Hydrol. Processes* **15** 1209–26
- Goolsby D A, Battaglin W A, Aulenbach B T and Hooper R P 2000 Nitrogen flux and sources in the Mississippi River Basin *Sci. Total Environ.* **248** 75–86

- Goolsby D A, Battaglin W A, Lawrence G B, Artz R S, Aulenbach B T, Hooper R P, Keeney D R and Stensland G J 1999 Flux and sources of nutrients in the Mississippi-Atchafalaya River Basin: Topic 3 report for the integrated assessment on hypoxia in the Gulf of Mexico NOAA Coastal Ocean Program Decision Analysis Series No. 17 (Silver Spring, MD: NOAA Coastal Ocean Program)
- Heisler J et al 2008 Eutrophication and harmful algal blooms: a scientific consensus *Harmful Algae* **8** 3–13
- Hurttt G C et al 2011 Harmonization of land-use scenarios for the period 1500–2100: 600 years of global gridded annual land-use transitions, wood harvest, and resulting secondary lands *Clim. Change* **109** 117
- Jeppesen E et al 2005 Lake responses to reduced nutrient loading—an analysis of contemporary long-term data from 35 case studies *Freshwater Biol.* **50** 1747–71
- Kreiling R M, Thoms M C, Bartsch L A, Richardson W B and Christensen V G 2019 Complex response of sediment phosphorus to land use and management within a river network *J. Geophys. Res.: Biogeosci.* **124** 1764–80
- Laurent A and Fennel K 2017 Modeling river-induced phosphorus limitation in the context of coastal hypoxia *Modeling Coastal Hypoxia* ed D Justic et al (Berlin: Springer) pp 149–71
- Lee C J and Reutter D 2019 Nutrient and pesticide data collected from the USGS National Water Quality Network and previous networks, 1963–2018 (U.S. Geological Survey Data Release)
- Li H, Wigmosta M S, Wu H, Huang M, Ke Y, Coleman A M and Leung L R 2013 A physically based runoff routing model for land surface and earth system models *J. Hydrol.* **14** 808–28
- Lindström G, Pers C, Rosberg J, Strömqvist J and Arheimer B 2010 Development and testing of the HYPE (hydrological predictions for the environment) water quality model for different spatial scales *Hydrol. Res.* **41** 295–319
- Liu J, You L, Amini M, Obersteiner M, Herrero M, Zehnder A J and Yang H 2010 A high-resolution assessment on global nitrogen flows in cropland *Proc. Natl Acad. Sci. USA* **107** 8035–40
- Maavara T, Chen Q, Van Meter K, Brown L E, Zhang J Y, Ning J R and Zarfl C 2020 River dam impacts on biogeochemical cycling *Nat. Rev. Earth Environ.* **1** 103–16
- Meade R H and Moody J A 2010 Causes for the decline of suspended-sediment discharge in the Mississippi River system, 1940–2007 *Hydrol. Processes* **24** 35–49
- Meybeck M 1982 Carbon, nitrogen, and phosphorus transport by world rivers *Am. J. Sci.* **282** 401–50
- Milliman J D and Syvitski J P 1992 Geomorphic/tectonic control of sediment discharge to the ocean: the importance of small mountainous rivers *J. Geol.* **100** 525–44
- Minaudo C, Curie F, Jullian Y, Gassama N and Moatar F 2018 QUAL-NET, a high temporal-resolution eutrophication model for large hydrographic networks *Biogeosciences* **15** 2251–69
- Mississippi River/Gulf of Mexico Watershed Nutrient Task Force 2015 *Mississippi River/Gulf of Mexico Watershed Nutrient Task Force 2015 Report to Congress* (Washington, DC: U.S. Environmental Protection Agency)
- Mitchell K E et al 2004 The multi-institution North American Land Data Assimilation System (NLDAS): utilizing multiple GCIP products and partners in a continental distributed hydrological modeling system *J. Geophys. Res.* **109** D07S90
- Mize S V, Murphy J C, Diehl T H and Demcheck D K 2018 Suspended-sediment concentrations and loads in the lower Mississippi and Atchafalaya rivers decreased by half between 1980 and 2015 *J. Hydrol.* **564** 1–11
- Montgomery D R 2007 Soil erosion and agricultural sustainability *Proc. Natl Acad. Sci. USA* **104** 13268–72
- Morgan R P C 2001 A simple approach to soil loss prediction: a revised Morgan-Morgan-Finney model *Catena* **44** 305–22
- Murphy J C 2020 Changing suspended sediment in United States rivers and streams: linking sediment trends to changes in land use/cover, hydrology and climate *Hydrol. Earth Syst. Sci.* **24** 991–1010
- Naipal V, Ciaia P, Wang Y, Lauerwald R, Guenet B and Van Oost K 2018 Global soil organic carbon removal by water erosion under climate change and land use change during AD 1850–2005 *Biogeosciences* **15** 4459–80
- Oleson K W et al 2013 *Technical Description of Version 4.5 of the Community Land Model (CLM)*; NCAR Tech (Boulder, CO: Note NCAR/TN-503+STR; NCAR) (<https://doi.org/10.5065/D6RR1W7M>)
- Peñuelas J et al 2013 Human-induced nitrogen–phosphorus imbalances alter natural and managed ecosystems across the globe *Nat. Commun.* **4** 2934
- Pimentel D and Kounang N 1998 Ecology of soil erosion in ecosystems *Ecosystems* **1** 416–26
- Pocklington R and Tan F C 1987 Seasonal and annual variations in the organic matter contributed by the St Lawrence River to the Gulf of St. Lawrence *Geochim. Cosmochim. Acta* **51** 2579–86
- Presley B J, Refrey J H and Shokes R F 1980 Heavy metal inputs to Mississippi Delta sediments *Water Air Soil Pollut.* **13** 481–94
- Rabalais N N, Turner R E, Justic D, Dortch Q and Wiseman J W J 1999 Characterization of hypoxia: Topic 1 report for the integrated assessment on hypoxia in the Gulf of Mexico NOAA Coastal Ocean Program Decision Analysis Series No. 15 (Silver Spring, MD: NOAA Coastal Ocean Program)
- Renard K G, Foster G R, Weesies G A, McCool D K and Yoder D C 1997 Predicting soil erosion by water: a guide to conservation planning with the revised soil loss equation (RUSLE) *Agric. Handbook* No. 703 (Washington, DC: U.S. Department of Agriculture) p 404
- Ricciuto D, Sargsyan K and Thornton P 2018 The impact of parametric uncertainties on biogeochemistry in the E3SM land model *J. Adv. Model. Earth Sys.* **10** 297–319
- Rostad C E, Leenheer J A and Daniel S R 1997 Organic carbon and nitrogen content associated with colloids and suspended particulates from the Mississippi River and some of its tributaries *Environ. Sci. Technol.* **31** 3218–25
- Runkel R L 2007 Toward a transport-based analysis of nutrient spiraling and uptake in streams *Limnol. Oceanogr. Methods* **5** 50–62
- Scavia D et al 2002 Climate change impacts on US coastal marine ecosystems *Estuaries* **25** 149–64
- Seitzinger S P et al 2010 Global river nutrient export: a scenario analysis of past and future trends *Glob. Biogeochem. Cycles* **24** GBOA08
- Smets T, Poesen J and Knapen A 2008 Spatial scale effects on the effectiveness of organic mulches in reducing soil erosion by water *Earth-Sci. Rev.* **89** 1–12
- Sutula M, Bianchi T S and McKee B A 2004 Effect of seasonal sediment storage in the lower Mississippi River on the flux of reactive particulate phosphorus to the Gulf of Mexico *Limnol. Oceanogr.* **49** 2223–35
- Sylvan J B, Dortch Q, Nelson D M, Maier Brown A F, Morrison W and Ammerman J W 2006 Phosphorus limits phytoplankton growth on the Louisiana shelf during the period of hypoxia formation *Environ. Sci. Technol.* **40** 7548–53
- Tan Z, Leung L R, Li H-Y and Tesfa T 2018 Modeling sediment yield in land surface and Earth system models: model comparison, development, and evaluation *J. Adv. Model. Earth Sys.* **10** 2192–213
- Tan Z, Leung L R, Li H, Tesfa T, Vanmaercke M, Poesen J, Zhang X, Lu H and Hartmann J 2017 A global data analysis for representing sediment and particulate organic carbon yield in Earth System Models *Water Resour. Res.* **53** 10674–700
- Tan Z, Leung L R, Li H, Tesfa T, Zhu Q and Huang M 2020 A substantial role of soil erosion in the land carbon sink and its future changes *Glob. Change Biol.* **26** 2642–55
- Tipping E, Somerville C J and Luster J 2016 The C:N:P:S stoichiometry of soil organic matter *Biogeochemistry* **130** 117–31
- US EPA 2009 National lakes assessment: a collaborative survey of the Nation's lakes *EPA 841-R-09-001* (Washington, DC: U.S. Environmental Protection Agency)

- US EPA 2013 National rivers and streams assessment (NRSA) 2008–2009 draft report *EPA/841/D-13/001* (Washington, DC: U.S. Environmental Protection Agency)
- USDA 2018 *Summary Report: 2015 National Resources Inventory* (Washington, DC: Natural Resources Conservation Service and Center for Survey Statistics and Methodology, Iowa State University)
- Van Meter K J, Van Cappellen P and Basu N B 2018 Legacy nitrogen may prevent achievement of water quality goals in the Gulf of Mexico *Science* **360** 427–30
- Vilmin L, Mogollón J M, Beusen A H W, Van Hoek W J, Liu X, Middelburg J J and Bouwman A F 2020 Modeling process-based biogeochemical dynamics in surface fresh waters of large watersheds with the IMAGE-DGNM framework *J. Adv. Model. Earth Syst.* **12** e2019MS001796
- Voisin N, Li H, Ward D, Huang M, Wigmosta M and Leung L R 2013 On an improved sub-regional water resources management representation for integration into earth system models *Hydrol. Earth Syst. Sci.* **17** 3605–22
- Ward N D, Bianchi T S, Medeiros P M, Seidel M, Richey J E, Keil R G and Sawakuchi H O 2017 Where carbon goes when water flows: carbon cycling across the aquatic continuum *Front. Mar. Sci.* **4** 7
- Yang X, Thornton P E, Ricciuto D M and Post W M 2014 The role of phosphorus dynamics in tropical forests—a modeling study using CLM-CNP *Biogeosciences* **11** 1667–81
- Zhu Q, Riley W J, Tang J, Collier N, Hoffman F M, Yang X and Bisht G 2019 Representing nitrogen, phosphorus, and carbon interactions in the E3SM Land Model: development and global benchmarking *J. Adv. Model. Earth Syst.* **11** 2238–58
- Zhu Q, Riley W J, Tang J and Koven C D 2016 Multiple soil nutrient competition between plants, microbes, and mineral surfaces: model development, parameterization, and example applications in several tropical forests *Biogeosciences* **13** 341–63